Experimental survey of the production of α-decaying heavy elements in ^{238}U + ^{232}Th reactions at 7.5–6.1 MeV/nucleon

S. Wuenschel,[1] K. Hagel,[1] M. Barbui,[1] J. Gauthier,[1] X. G. Cao,[2,1] R. Wada,[1] E. J. Kim,[1,3] Z. Majka,[4] R. Płaneta,[4] Z. Sosin,[4,*] A. Wieloch,[4] K. Zelga,[4] S. Kowalski,[5] K. Schmidt,[5] C. Ma,[6] G. Zhang,[2] and J. B. Natowitz[1]

[1]*Cyclotron Institute, Texas A&M University, College Station, Texas 77843, USA*

[2]*Shanghai Institute of Applied Physics, Chinese Academy of Sciences, Shanghai 201800, China*

[3]*Division of Science Education, Chonbuk National University, 567 Baekje-daero Deokjin-gu,Jeonju 54896, Korea*

[4]*M. Smoluchowski Institute of Physics, Jagiellonian University, PL-31-007-Krakow, Poland*

[5]*Institute of Physics, University of Silesia, PL-40-007 Katowice, Poland*

[6]*Institute of Particle and Nuclear Physics, Henan Normal University, Xinxiang 453007, China*

(Received 12 February 2018; published 4 June 2018)

The production of α-particle decaying heavy nuclei in reactions of 7.5–6.1 MeV/nucleon ^{238}U +^{232}Th was explored using an in-beam detection array composed of YAP scintillators and gas ionization chamber-Si telescopes. Comparisons of α energies and half-lives for the observed products with those of the previously known isotopes and with theoretically predicted values indicate the observation of a number of previously unreported α emitters. α-particle decay energies reaching as high as 12 MeV are observed. Many of these are expected to be from decay of previously unseen relatively neutron rich products. While the contributions of isomeric states require further exploration and specific isotope identifications need to be made, the production of heavy isotopes with quite high atomic numbers is suggested by the data.

DOI: 10.1103/PhysRevC.97.064602

I. INTRODUCTION

The synthesis of and the characterization of the properties of heavy and super-heavy elements is one of the important current focal points in both experimental and theoretical nuclear science. Very high atomic number nuclei have long been predicted to exhibit new stabilizing shell structures as well as possible exotic shapes such as toroids and bubbles. See Refs. [1–9] and those within. Studies of the chemical properties of new heavy elements are being employed to establish their chemical families and serve to provide stringent new tests of our understanding of relativistic effects in electron structure [10–13].

Model predictions for a shell stabilized "island of stability" differ in the locus of the center of that island, but agree in their prediction that the fission barriers in the island region reduce the probability of fission during de-excitation of the primary excited nuclei produced in synthesis reactions and mitigate against the spontaneous fission decay mode of those isotopes [14–24]. Thus the main modes of decay in and near these islands are predicted to be α and β decay [15–17,22–24].

The synthesis technique which is typically used to search for new heavy isotopes is fusion of a heavy target nucleus with a light to medium projectile nucleus [5,6,25–31]. The compound nuclei formed have excitation energies which favor fission into two medium mass nuclei rather than gentler sequential emission modes. As a result the net production probability for heavy nuclei which survive fission usually decreases rapidly with increasing atomic number of the fused system [25–31].

Fusion of doubly magic neutron-rich ^{48}Ca projectiles with trans-uranium target nuclei has led to the synthesis of elements as high as $Z = 118$ [25–31]. For the reaction used to produce element 118, oganesson, the reaction cross section using ^{48}Ca is ∼0.5 picobarns [25–27]. Such cross sections severely limit the prospects for heavy element research. Even when the projectiles are neutron rich the compound nuclei produced are neutron deficient relative to the line of β stability.

The limitations of fusion reactions have led to a renewed interest in exploring alternative reaction mechanisms for production of neutron-rich heavy and super-heavy isotopes. In particular considerable theoretical effort was devoted to exploring the use of multinucleon transfer reactions between pairs of heavy nuclei [32–41]. This technique received some earlier attention from both experimentalists and theorists [42–51] but, based on the early experimental results was not pursued for heavy element synthesis.

Recent new approaches employed to model the initial multinucleon transfer stage of such reaction processes typically calculate yields and excitation energies of primary isotopes and then employ statistical decay models to predict the final product distributions resulting from the ensuing de-excitation stages [32–37]. Fission is, of course, the key competing de-excitation mode which limits the heavy isotope survivability and spontaneous fission can compete directly with α or β decay. Predicted fission barriers and α-decay energies rely upon model-dependent mass surface extrapolations [15–24]. The predicted survival cross sections for heavy and super-heavy nuclei are extremely sensitive to details of these mass surface

[*]Deceased.

extrapolations and the location of closed shells. Uncertainties of 1 MeV in the fission barriers can lead to an order of magnitude change in the fission probabilities. Uncertainties in level densities, temperature dependencies of fission barriers, and details of the fission dynamics further complicate calculations of fission probabilities. While quantitative predictions vary widely, systematic theoretical studies of survival probabilities carried out using both statistical models and microscopic model calculations of fission rates indicate high survival probabilities in and near the island of stability [15–17,20–24]. Notably, recent microscopic fission model results indicate significant increases in fission survivability compared to those of statistical models employing the same fission barriers [52,53]. Indeed, a strong increase in survivability is already evident in the experimental fusion cross-section data for the heaviest elements [28–31].

Some calculations suggest that near the valley of stability, β decay competes with α and fission decay and that short-lifetime β minus decay will be dominant for the more neutron-rich isotopes in that region [22–24]. This raises the interesting possibility that the production of neutron-rich lower Z products can feed higher Z products through β^- decay, increasing the effective production cross section for such higher Z products near the line of stability. Recent systematic efforts to explore the utility of multinucleon transfer reactions for production of new neutron-rich isotopes suggest that the experimental cross sections exceed predicted cross sections [38–41]. It is interesting to ask whether a similar trend exists for heavier elements. Good experimental data are needed to guide future efforts in heavy element research.

II. EXPERIMENTAL PROCEDURE

In some earlier work on this problem we used the BigSol Superconducting-Solenoid Time of Flight Spectrometer at Texas A & M to perform several surveys of projectile target combination and bombarding energy for collisions of ^{86}Kr, ^{136}Xe, and ^{197}Au with ^{232}Th in an effort to identify good candidate reactions for heavy and super-heavy element production [54–58]. Those experiments, at higher laboratory energies per nucleon than the present work, indicated the possible production of heavy elements with Z above 100 [58]. However, the experiment was discontinued when the spectrometer developed a He leak which made it not possible to sustain the necessary magnetic field. We then adopted a new direction for investigation of such reactions based upon the implantation of heavy reaction products in a downstream catcher foil and the detection of α-particle decays characteristic of heavy nuclei. For this purpose the Jagellonian University Group constructed a forward array of 63 active catcher (AC) fast plastic scintillator detectors and dedicated state-of-the-art fast timing electronics to function as a time filter for recoil implantation and α-decay detection [57,58]. Tests employing these plastic scintillators demonstrated that the use of such a time filtering device was feasible even in the harsh environment encountered in the experiments envisaged. The test experiments indicated a possible production of α-decaying heavy elements. However, while the fast plastics provided optimum time resolution, the quenching of the light-output inherent in solid scintillators and

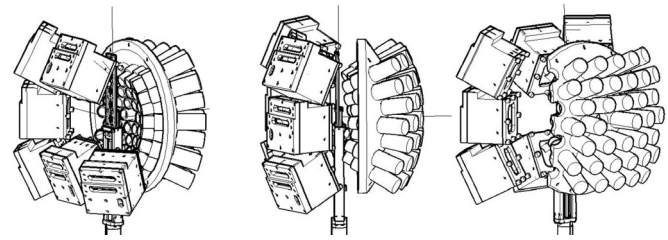

FIG. 1. Schematic diagram of IC-Si detectors and YAP active catcher array. The three views are from three different angles. In the central view the beam enters from the left.

the inability to do pulse shape discrimination with the plastic meant that discrimination between high-energy α particles and spontaneous-fission fragments was difficult.

Therefore, to carry out the present experiments we constructed an active catcher system consisting of a 40-detector array of yttrium aluminum perovskite (YAP) scintillators coupled to Hamamatsu photomultiplier tubes (PMTs) via Lucite light guides; see Fig. 1. The YAP scintillators were chosen because of the fast rise time and light decay properties ($t_1 \sim 14$ ns, $t_2 \sim 140$ ns) that provide access to particle identification through pulse shape discrimination. This capability is employed to distinguish between α decay and fission fragments or degraded beam and recoiling reaction products. This is important because the nonlinear response of the solid YAP scintillator makes energy signals alone insufficient for complete separation. The particle identification is demonstrated in Fig. 2 where we plot the slow component of the light versus the fast component. The gates for the different identified products are shown on the plot. The PMTs were powered by custom made active bases. The active bases provide the capacity to handle ~100× more events/second than the Hamamatsu

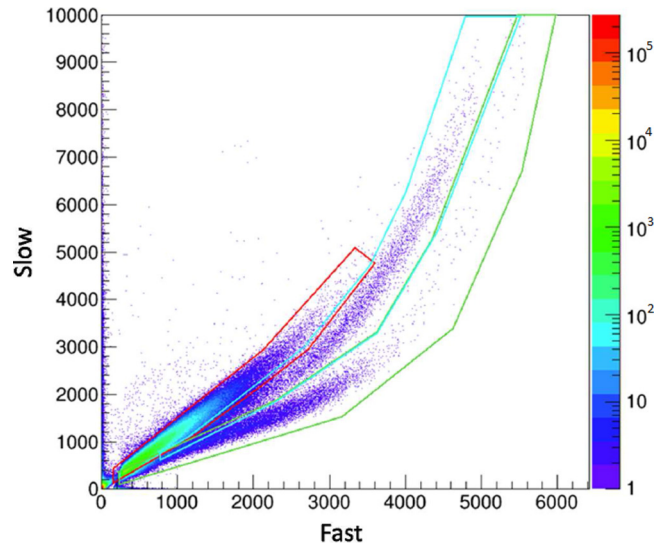

FIG. 2. Pulse-shape discrimination. Amplitude of slow portion of the AC signal vs amplitude of the fast portion (peak) signal. Windows indicated are, from left to right, α particles, fission fragments, and beam and heavy recoils. Data for both beam-on and beam-off are included.

passive bases before PMT gain sagging becomes an issue [59]. This resulted in additional beam intensity capacity. During offline testing, the active catcher modules (YAP-light guide PMT) exhibited $<10\%$ resolution for the 8.78-MeV α-decay peak of ^{228}Th. In the experiment the array had a total geometric efficiency of 22% for forward-recoiling products in the angular range of 7–60 degrees. As noted below the experiments reported in this paper were carried out in a pulsed beam mode. Derived implantation depths for the recoils ranged from a few microns to ∼18 microns. As a result, the intrinsic detection efficiency for the α decays in the AC was $>50\%$ (depending upon implantation depth). This is a direct reflection of escape effects which significantly reduces the ability to detect parent-daughter correlations in the AC alone. As employed the AC array was sensitive to products with transit times of only a few nanoseconds (much shorter than those of spectrometer experiments) originating from various reaction mechanisms. This array was employed with a backward array of gas ionization chamber-silicon telescopes (IC-Si) capable of detecting α particles emerging from the forward catcher; see Fig. 1.

An annular ring shielded the IC-Si telescopes from emission from the target. This IC-Si telescope array, active in both beam-on and beam-off modes had an overall geometric efficiency of 6% for α's originating in the active catcher and an α-particle identification threshold of 5.6 MeV. In addition to providing detection and identification of the α particles emerging from the YAP array, the coincidence capability thus realized provides a reconstruction of total α energy for those emerging α particles detected in the backward direction as well as information on implantation depth. The SRIM range-energy code was used to derive the required range-energy information for the implantation depth calculations [60]. In the experiment implantation depths of 2–22 microns were observed for accepted coincident α particles. These particles had total energies as large as 12 MeV. Some apparently higher energy α particles were observed by the IC-Si detector. These had unphysical apparent depths and were attributed to long-range α's from ternary fission with attendant larger AC coincidence energies resulting from simultaneous detection of fission fragments.

During the experiment one of the IC-Si detectors was blinded by a thick degrader. This allowed us to evaluate possible spurious events which might arise from (n,α) reactions in the detector materials. This effect was found to be negligible, consistent with GEANT simulations of this possibility [61].

The time decay constants inherent in YAP scintillators are notably slower than the fast plastic utilized initially. Thus, the dedicated, custom-made electronics and trigger scheme employed for the plastic scintillator array could not be easily adapted to these detectors. For this reason we turned to commercially available electronics for the YAP array. An experimental setup employing a triggering and signal acquisition scheme based upon the Struck SIS3316 250-MHz Flash ADC modules was developed. These modules provide flexible digital triggering mechanisms.

Although the direct catcher technique does require us to work in a somewhat hostile environment, it has an advantage relative to the spectrometer in the much shorter transit times of the recoils. Typical target to catcher flight times, and thus implantation times, were ∼5 ns. This means that activities with much shorter lifetimes can be investigated. We emphasize that the present experiment was intended to provide a broad-based survey and could be followed up by more targeted experiments guided by these results.

In July 2016, experimental data were taken using the YAP active catcher array coupled to the backward angle IC-Si detector modules. Beams of ^{197}Au and ^{238}U of 7.5 MeV/nucleon were incident on 11 mg/cm^2 ^{232}Th targets. The beam emerged from this target with an energy well below the Coulomb barrier of 6.1 MeV/u.

The trigger scheme employed in these experiments was based on three operational considerations:

(1) The experiment could be carried out in a pulsed beam mode with variable beam-on/beam off times.
(2) The backward angle silicon detector modules generate triggers at a relatively low rate and very high quality.
(3) Vetoing beam-on signals with the RF signal would have allowed the SIS3316 modules to trigger in a mode very similar to the Jagellonian University analog electronics. However, because the RF signal is about 5-ns wide, the Flash ADC bins are 4-ns wide, and the YAP signals are about 5-ns wide, the convolution of these signals did not allow to trigger closer than 17 ns from the RF signal which meant that such operation would have required vetoing about 30% of the time.

To avoid the problems associated with point 3, we decided, in this experiment, to allow the forward angle YAP detectors to trigger acquisition only during the beam-off periods.

Triggering of the acquisition utilized two primary modes, beam-on and beam-off. During the beam-on periods, only the silicon detectors triggered the acquisition. The active catcher array was read in slave mode and waveforms were stored for 2 μs for each active catcher module. The synchronization between Si and YAP was set so that a coincident peak in an active catcher module would appear at ∼790 ns into the 2-μs flash ADC storage period. During the beam-off periods, the active catcher detectors were permitted to trigger the acquisition. Waveforms were stored only for modules that triggered during the event. Because the trigger was generated entirely digitally, the beam-on or beam-off trigger mode was swapped using beam-on or beam-off bits provided to the acquisition system. During this experiment two different pulsing patterns were employed; 100-ms beam-on—30-ms beam-off and 30-ms beam-on—30-ms beam-off.

A third overarching trigger was also built into the logic. This intermittent trigger was applied to the silicon detectors. The SIS3316 modules have a binary threshold mode. The secondary threshold can be used to either veto an event, or as in our case, generate a secondary logic signal routed to another lemo output. The threshold for this trigger was set to 8–8.5 MeV energy in the silicon detectors. Following an event generating this second, high-energy trigger signal, the beam was completely turned off for 20 s and the acquisition set into the beam-off trigger mode. Additionally, for such events, the flash ADC storage periods were extended to be 160-μs long.

Using the multiple trigger modes it was possible to efficiently explore α spectra during beam-off periods of 2 μs, 160 μs, 30 ms, and 20 s and beam-on periods of 100 ms and 30 ms. Dead times were determined by the computer acquisition system dead time. In a typical experimental run the beam-on counting rate was ∼150 events/s. The addition of AC triggering with beam-off produced rates of about 300 events/s. As a result, the beam-on dead time was ∼38% and beam-off dead time was ∼75%.

Our original intention for beam monitoring for cross-section determinations was to use active catchers at larger angles to directly count elastically scattered particles. The change in triggering for the YAP detectors prevented this so beam monitoring was done using a Faraday cup in the fringe field at the exit port of the accelerator.

For the data analysis an offline peak finding algorithm was developed based on the trapezoidal digital filter used in the SIS3316 triggering process. The response of this algorithm also generated the fast portion of the pulse shape discrimination. A minimum of 20–40 ns separation results from the settings chosen for this algorithm which were optimized for YAP and the 4-ns buckets of the FADC. Currently, deconvolution of peak pile-up is not built into the analysis package. This creates an effective minimum distance between particle identified peaks of approximately 80–100 ns. This leads to a lower limit of 10^{-7} s for half-life determinations in this experiment. Tests with 40-ns minimum distances revealed little change in acceptance rates. Pile-up of pulses separated by less than 16 ns could result in errors in derived peak energies. Visual inspection of high-energy peaks of interest was employed to exclude this possibility.

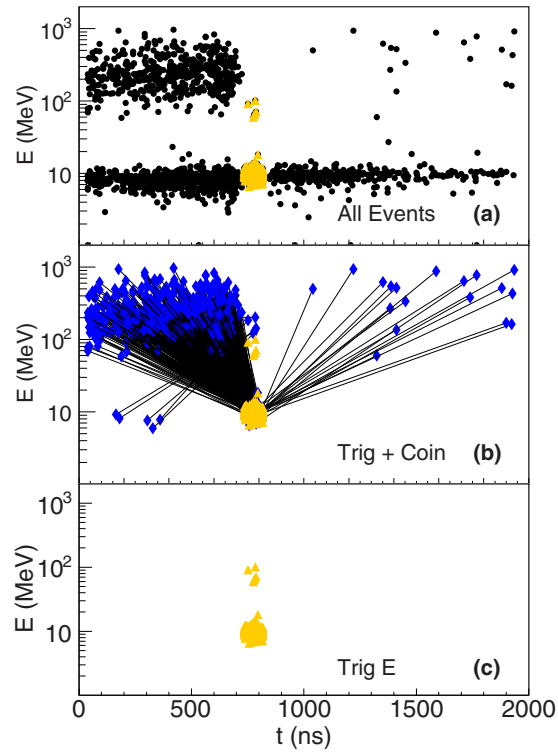

FIG. 3. Recorded energies and times for IC-Si triggered events having more than one AC signal in the 2-μs Flash ADC inspection time. Events are for detectors in the angular range of 30–50 degrees. IC-Si triggers appear at ∼790 ns. Lines indicate the correspondence between α-particle signals and heavy product signals observed in the same 2-μs period. (a) All events; (b) coincident heavy product α-particle events; (c) trigger events. See text.

III. ANALYSIS AND EXPERIMENTAL RESULTS

As a first result from the experiment, we present in Fig. 3, a plot of assigned energies (AC or IC+ Si+AC) for events in which more than one flash ADC signal was registered in the 2-μs recording window associated with an IC-Si trigger.

The actual trigger signals appear at ∼790 ns in this plot. While most of these events have one other peak, some have two. Thus in the plot we see energies of other α particles detected in the AC during the inspection period. We also see a number of much higher energy signals. The overwhelming number of these signals precede the trigger. In the figure we have also included lines connecting each of these high-energy signals to α-particle signals seen in the same AC module during the same 2-μs Flash ADC recording period. We conclude that these signals correspond to the implantation of heavy α-decaying recoils which precede the trigger decay within the 2-μs window. Further confirmation of this is that we have observed target to catcher flight times and recoil energy-implantation depth correlations (derived from the energy loss of the α particles emerging from the AC) which are consistent with the energies assigned. The recorded recoil to trigger flight times are employed in a later section to determine apparent half-lives for this subset of events.

We also note in Fig. 3 several trigger events with total energies ∼100 MeV. These events correspond to detection of an identified α particle in the IC-Si associated with a signal identified as fission in the AC (the fission energy calibration is only approximate). These appear to correspond to ternary fission events emitting long-range α particles [61].

We present in Fig. 4 a comparison between energy spectra of the Si-IC detected events (including a window correction), of the AC detected events, and of the combined IC-Si-AC detected events. The agreement between the last two is very good, providing important confirmations of the individual detector calibrations and the pulse shape identification techniques employed to identify α particles in the YAP detectors.

A careful exploration of the IC-Si trigger events using their apparent implantation depths indicated that identified α particles with total energies above ∼11.5 MeV corresponded to α emission in ternary fission events or included possibly misidentified YAP signals at the limit of our pulse shape discrimination capabilities. Therefore in the analyses reported below we have limited ourselves to identified α particles with energies $\leqslant$11.5 MeV.

The resolution of the YAP detectors is such that resolving emission from individual isotopes in the midst of the large number of isotopes with similar α-decay energies is extremely difficult. Thus we have instead elected to explore overlapping sequential bins of α energy, 400-keV wide, displaced each time by 200 keV to survey the dominant decay times as a function of energy. These fits were restricted to average energies below 11.5 MeV, based upon the implantation depth information described above.

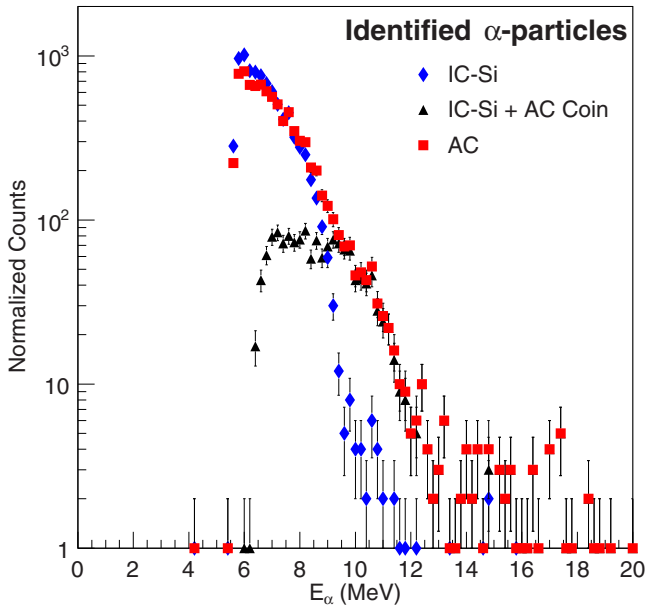

FIG. 4. Comparison of α-particle kinetic energy spectra. (Diamonds) Energy spectrum in IC-Si telescope including window correction; (triangles) energy spectrum sum of IC-Si energy plus coincident AC energy; (squares) energy spectrum in AC detector. The last two spectra are normalized at 10 MeV.

For each energy bin we employed the method suggested by Schmidt *et al.* to explore decay time distributions [62]. For a given decaying nucleus the decay time distribution data is characterized by a universal function. In the fitting parent-daughter relationships which exist are not explicitly taken into account. This, and the limitations of the three-source assumption mean that the fit results are primarily indicative of the decay times of the nuclei whose yields are dominant in a sampled energy range. We return to the question of parent-daughter relationships later in this paper. The universal function is given by

$$\frac{dn}{d\theta} = n\lambda e^{\theta} e^{-\lambda e^{\theta}}, \tag{1}$$

in which $\theta = \ln t$ where t is the decay time and the free parameters are n, the total number of counts, and $\lambda = 1/\tau$ where τ is the mean lifetime. The most probable value of this distribution is $\ln \tau$. We have employed this function as a fitting function to explore the decay curves as a function of α energy in each time region. Implicit in this approach is that the times are generally measured from the beginning of the decay period explored. However, in the particular case of the 2-μs and 160-μs flash ADC recording periods, we have observed recoil-α-particle coincidences. For such events the times are those between recoil and α-particle detection. Corrections for recoil and α flight time differences are small.

Figure 5 shows an example of the fitting strategy pursued. In that figure the results of three-source fitting for bins of mean energy ranging from 6.8 to 10.2 MeV are shown. The three sources are qualitatively identified as fast, medium, and slow. The derived values of the mean lifetimes τ, and normalization constants n, are plotted as a function of mean energy.

In Fig. 6, we summarize the results of this investigation, plotting half-life in seconds vs the α-particle kinetic energy in MeV. The apparent clustering into seven dominant time ranges reflects weighted averages of the activities falling within the selected α-particle energy windows for the three-source approximation and the pulsing protocol chosen. A different pulsing protocol would lead to different relative weightings of the activities included and the three-source fits could emphasize different time ranges. For later discussion, we identify these groups as group 1 to group 7 in order of decreasing half-life range (top to bottom).

For comparison to the data we present three other sets of information. The first set, indicated by open circles, represents the experimental data for $t_{1/2}$ vs α energy for previously identified α-decaying isotopes with $Z \leqslant 101$ [64]. The second, indicated by closed triangles represents the existing experimental data for elements heavier than 101 [64,65]. The third set, represented by solid squares connected by lines, indicates the values calculated for partial α-decay half-lives for even-even isotopes with Z from 98 (Cf) to 130 (left to right) and N from 172 to 196 using a density-functional approach with the PCPK3 interaction [18]. As is commonly done, the authors calculated these partial half-lives employing the usual Viola-Seaborg approach with parameters determined from fits to the known isotopes [66].

Various predictions for the branching ratios for the decay of the heaviest of the elements in the region of the valley of stability strongly favor α emission [16,17,22]. Significant contributions from other decay modes would lead to smaller total half-lives for the nuclei considered. For even-odd (E-O), odd-even (O-E), and odd-odd (O-O) nuclei traditionally invoked hindrance factors for α decay would lead to some increases in the partial α-decay half-lives compared to those of the neighboring E-E isotopes [15].

Theoretical calculations of fission barriers and fission lifetimes have also been carried out for heavy and super-heavy elements [16,17,19–22]. In Ref. [16] Staszczak *et al.* have calculated both α decay and spontaneous fission lifetimes for a similar, but more limited, set of even-even heavy nuclei than considered in Ref. [18]. In Fig. 7, the total half-life predictions of Staszczak *et al.* [16] are compared to the partial α-decay lifetimes of Agbemava *et al.* [18]. The fission competition included in the first often leads to large (many orders of magnitude) reductions in the predicted lifetime. The largest changes are in the 8–10 MeV energy region, reflecting larger predicted branching ratios for spontaneous fission. A number of sub-nanosecond activities are predicted. Given significant branching ratios for spontaneous fission it is possible that the experimentally observed sub-millisecond activities in Fig. 7 correspond to higher Z isotopes than the comparison to partial α half-lives alone would suggest.

The data in Fig. 6 indicate the observation of a number of previously unreported α emitters with energies reaching as high as 11.5 MeV. Given the multinucleon transfer mechanism in play many of these are expected to be previously unseen neutron-rich products. The raw comparison between data and predictions in the millisecond and second time ranges shows α-particle energies which might represent decay from very high Z isotopes. However, we must recognize that α particles emitted

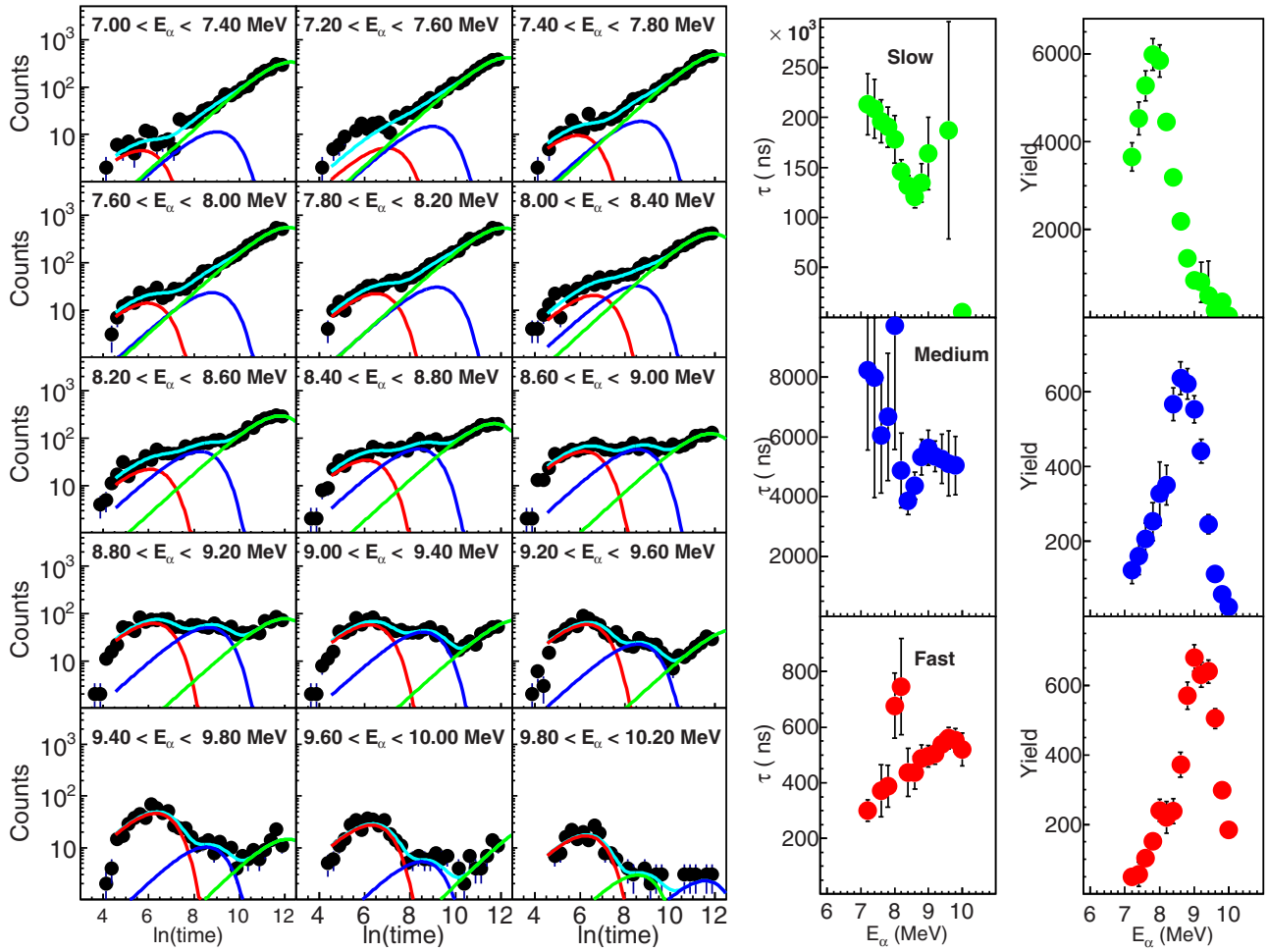

FIG. 5. Example of fitting process results. On the left the results of fitting the function of Eq. (1) to α-energy selected data from the millisecond pulsing range are shown. Data, solid circles; source fits, lines. On the right are derived mean lifetimes and yields from the three component fits versus the average of the selected bin.

from new isomeric states can have energies quite different from those of their ground-state counterparts and thus would lead to a different $t_{1/2}$ energy correlation. This is well established in the Fr-At region, for example [64].

Although the experimental α-energy resolution (FWHM $\sim$ 600 KeV) coupled with the high decay rates observed make searching for individual decay chains difficult, we can make an initial test of the isomer hypothesis by asking, on an event-by-event basis, what energies are observed following emission of an initial α particle of ever increasing energy. For events in which the beam was turned off for 20 s we present, in Fig. 8, the energy differences ($E_{\text{subsequent}}$-E_{initial}) vs E_{initial} where E_{initial} is the energy of the first α detected in the event and $E_{\text{subsequent}}$ are the energies for the next four α particles detected in the same active catcher module. A lower threshold of 9.5 MeV was imposed on the initial α-particle energies used for this search.

Up to $\sim$10.6 MeV initial energy the observed energy differences span an energy range of about 2 MeV and include particles with energies within $\sim$0.5 MeV of the initial energy. At higher energies the band narrows and by an initial energy of 11 MeV most subsequent α particles have energies more than 1.5 MeV lower. This is generally larger than predicted (and observed) differences in energies of successive ground-state decays. The populating of α-decaying isomeric states could explain this observation. Near 11.5 MeV initial energy single events with subsequent energies 1.2 and 1.4 MeV lower than the initial energy bear further investigation. Of course isomeric states can also contribute at lower decay energies. To determine the actual identities of the high α-energy emitters and resolve the question of isomer contributions to our spectra requires that detailed decay chain relationships be established.

IV. PARENT-DAUGHTER RELATIONSHIPS

We have attempted searching for parent-daughter relationships by applying energy-energy correlation methods analogous to those used in gamma-decay spectroscopy [67]. Two powerful peak searching software packages were employed [68,69]. As previously noted, and emphasized by the correlation plot shown in Fig. 9, the high rates of α decay in a single AC module coupled with the energy resolution of the present

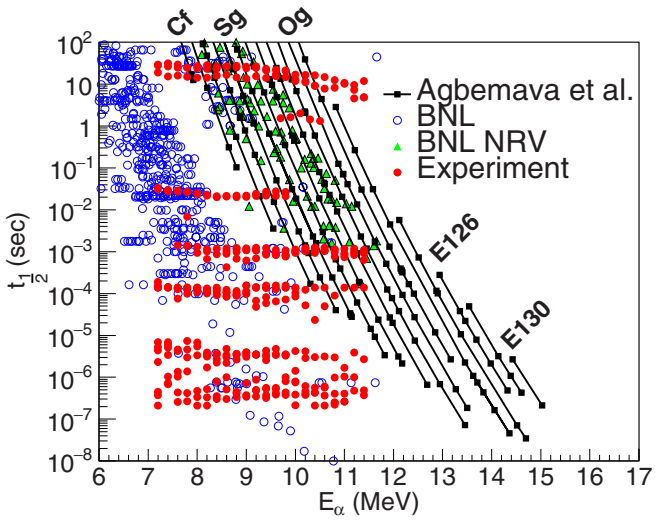

FIG. 6. Grand summary. Total half-life, seconds vs E_α, MeV for activities with $t_{1/2} \leqslant 100$ s. (Open circles) Known α half-lives for isotopes with Z to 101 [64]; (solid diamonds) NRV [65] and BNL [64] data for isotopes with $Z > 101$; solid black squares connected by lines depict predictions of partial α lifetimes vs E_α for even-even nuclei, left to right $Z = 98$–130. Data for different time ranges are represented by closed circles (see text). There are seven separated groups of data. The group of data having the longest half-lives (near the top of the plot) is denoted as group 1. Group 7 is the group of data having the shortest half-lives. Half-lives were derived for moving α-particle energy bins of 0.4 MeV. Thus the experimental points are equally spaced on the energy axis. Statistical uncertainties on the fitted half-lives are of the order of the spread seen in the different time bands.

experiment make peak searching difficult. Improvements in detector resolution and granularity would greatly improve the peak search capabilities.

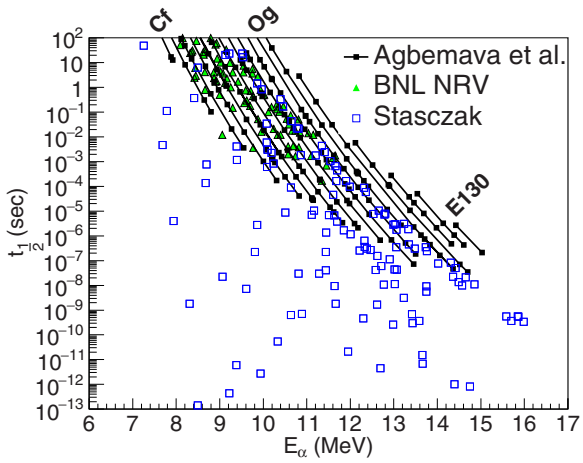

FIG. 7. Comparison of the predicted partial α-decay half-lives for even-even isotopes (filled squares) [18] with predicted total half-lives including spontaneous fission (open squares) [16]. Also shown are known experimental half-lives tabulated in the BNL [64] and NRV [65] data bases (filled triangles). The theoretical calculations represented cover ranges of atomic number of Z=101–130 and N =142–196. See references for details.

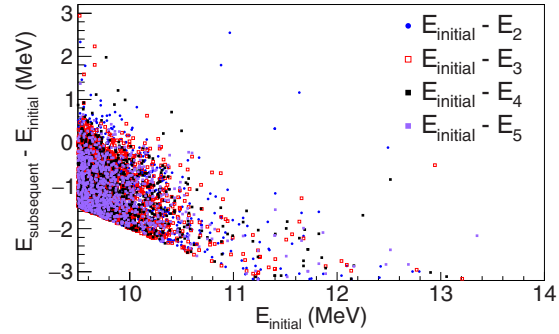

FIG. 8. For 20-s beam-off data, energies of α particles emitted following an initial α particle with $E \geqslant 9.5$ MeV. See text.

Nevertheless, during these attempts we did isolate, for the 20-s beam-off events, some statistically significant correlated emission pairs indicating parent-daughter relationships. Half-lives for the daughters could be determined from the measured time differences.

Half-lives in the 1- to 2-s range are observed for α-particle kinetic energies of 9.3–10.3 MeV. These results are presented in Table I. In Fig. 10 they are compared with previously reported literature results [63,64] and with the theoretical predictions for even-even nuclei from Ref. [18].

While theoretical predictions for Q_α and $t_{1/2}$ for a specific super-heavy isotope vary significantly [16–18], the phenomenological trends for fixed atomic number, based on the Viola-Seaborg approach [66] and represented by the lines for even-even nuclei in Fig. 10, are quite robust. The comparison to the theoretical results suggests that, if these emitters are even-even nuclei, they are in a range of Z from 106 to 114. Recall that these are the daughter nuclei in the correlated α-particle pairs. The parent nuclei would have atomic numbers 2 units higher than the daughters. For even-odd, odd-even, and odd-odd nuclei the inclusion of phenomenological hindrance factors leads to predicted half-lives ∼2 to 10 times longer than those for E-E nuclei of the same atomic number. Thus further information is required to make definitive atomic number and isotope identifications.

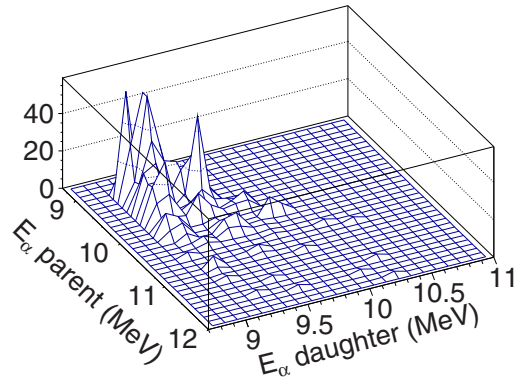

FIG. 9. 2D energy-energy correlation plot for data taken during 20-s beam-off periods.

TABLE I. Correlated pair half-lives.[a]

α emission			Spontaneous fission	
Parent α energy (MeV)	Daughter α energy (MeV)	$t_{1/2}$ Daughter (s)	Parent α energy (MeV)	$t_{1/2}$ Fission (s)
9.29	9.12	1.49 ± 0.32	8.15	1.86 ± 0.28
9.63	9.45	1.16 ± 0.36	8.45	1.28 ± 0.17
9.75	9.12	1.35 ± 0.38	8.97	0.74 ± 0.35
9.88	9.72	1.20 ± 0.21	9.19	1.22 ± 0.27
9.92	9.36	0.96 ± 0.26	9.45	2.18 ± 0.37
10.04	9.09	0.99 ± 0.55	10.05	1.83 ± 1.08
10.14	9.88	0.99 ± 0.32		
10.26	9.51	1.13 ± 1.18		

[a]Search with ± 0.15-MeV standard deviation on α energies.

V. SPONTANEOUS FISSION

The same energy-energy correlation techniques used to search for α-α correlations were used to search for spontaneous fission decays following α emission. In this search we identified some α-fission correlated pairs with parent α energies ranging from 8.15 to 10.1 MeV. The spontaneous fission daughter half-lives were also found to be in the few second range. These results are also summarized in Table I.

VI. CROSS SECTIONS

To determine cross sections from the three-source fit results we have assumed that a secular equilibrium with the beam is achieved for each activity which is short relative to the relevant pulsing time. In this case the normalization constant of the fitting function is the number of nuclei present when the beam is turned off (integrated over the number of pulsing cycles). With the secular equilibrium assumption the cross sections are easily derived. In Fig. 11 we show thick target differential cross sections as a function of α-particle energy for the 20-s beam-off events in group 1.

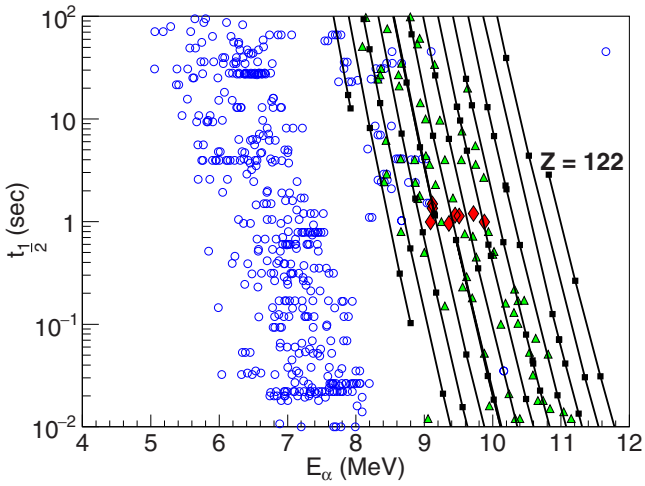

FIG. 10. Experimental results of correlated pair search (solid diamonds). For comparison data from previous experiments are shown. Open circles denote $Z \leqslant 101$ [64] and filled triangles denote $Z > 101$ [65]. The predictions of Agbemava *et al.* [18] for E-E nuclei with $Z = 98$–122 are indicated by filled squares connected by lines to guide the eye.

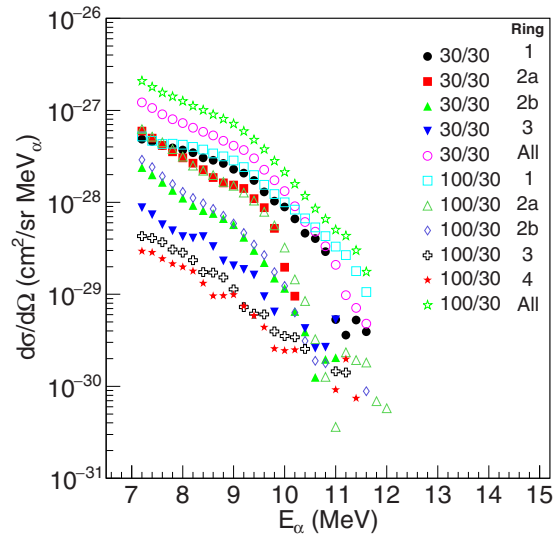

FIG. 11. Integral thick target differential cross sections cm^2/sr MeV vs α-particle energy. Angular ranges are Ring 1 (16°–30°), Ring 2a (31°–45°), Ring 2b (36°–50°), Ring 3 (47°–51°), Ring 4 (52°–66°). The beam pulsing (beam-on—beam-off times in ms) configurations for the various symbols are indicated in the legend.

It is important to emphasize that the average cross sections for these α-energy ranges are derived from integral thick target production rates assuming that the entire energy range from incident beam energy down to the Coulomb barrier is contributing. They include all feeding from parent activities during the irradiation. In addition, the energy resolution is such that more than one isotope will contribute in the selected energy windows.

The strong decrease of cross section with increasing α energy is consistent with the general trend of increasing Z with increasing α energy and qualitatively consistent with the trend predicted by multinucleon transfer models. In this case the production of lower energy activities, while having contributions of feeding from higher Z, will tend to be dominated by direct production.

The differential cross sections seen in Fig. 11 depend upon α energy, half-life, and detection angle. The mixture of activities in a given α-energy range also can depend on pulsing protocol. As the bulk of the data appear in the ring 2 portion of the active catcher we have chosen that ring, which spans an angular range 31°–50°, for comparison of the differential cross sections for different half-life ranges. As previously noted in Figs. 6 and 7 different bands of sampled half-lives are observed. We identified these, from top to bottom, as bands 1–7. In Fig. 12 we present the measured thick target differential cross sections for ring 2 for each of these bands.

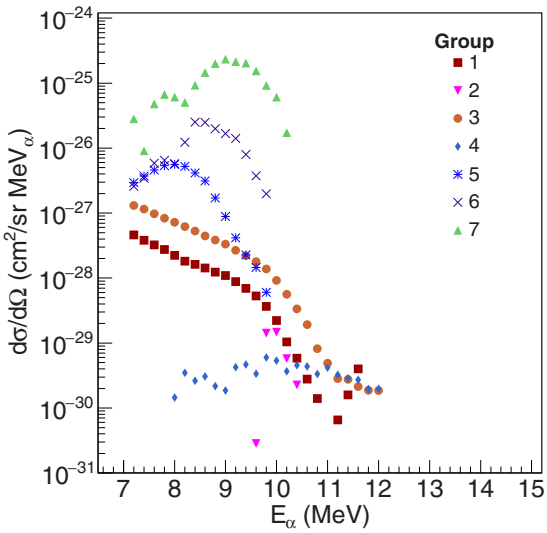

FIG. 12. Thick target differential cross sections, cm^2/sr MeV in angular range 31°–50°. See text.

VII. COMPARISON TO PREVIOUS RESULTS

In the late 1970s several groups employed similar multinucleon transfer reactions at energies ranging from the Coulomb barrier to 8.5 MeV/nucleon to search for new elements from super-heavy elements [43–50]. These included both in-beam detection and radiochemical studies seeking evidence of new spontaneously fissioning or α-emitting nuclei. Both thin target and thick target irradiations were carried out. In all cases no new elements were observed and half-life dependent upper limits to heavy element production cross sections were reported.

The present data for thick target cross sections indicate cross sections which are somewhat in excess of those limits. It is natural, therefore, to ask why this is the case. For the previous radiochemical and gas jet experiments thick targets were employed. Time delays inherent in the radiochemical and jet techniques might account for some of the present differences. Reference [49] also reports results of a rotating wheel collection experiment, but only to search for spontaneous fission activities. We speculate that implantation depths of the products may have had some effect on the results reported.

The previous experiment which may be most directly compared with ours is the in-beam experiment of Refs. [43,46]. One significant difference is that their experiment employed a thin target so that a very small range of reaction energy at 7.42 MeV/u was explored. In contrast our experiment explores the range from 7.5 MeV/u down to ∼6 MeV/u. Inspection of the α-energy spectra in Ref. [46] reveals low level high-energy signals which could be candidates for heavier element decay but were discounted because the microsecond time resolutions in the experiments did not allow sufficient discrimination against pile-up events. The α spectrum presented in Ref. [45] also shows some potentially interesting α particles below 11.6 MeV. For energy above that the observed signals from two experiments for a total beam time of 5.5 h indicate pile-up contributions similar to those invoked in Ref. [46]. In the present experiment modern flash ADCs were operated in a mode which allowed ∼16-ns time resolution, greatly reducing pile-up possibilities. In addition, the recording of the individual detector signal traces allowed inspection of individual detector signals. Our analysis was restricted to events with flash ADC signals separated by 40–100 ns.

VIII. SUMMARY AND CONCLUSIONS

The present experimental results for a survey of the production of α-particle decaying heavy nuclei in reactions of 7.5–6.1 MeV/nucleon $^{238}U + {}^{232}Th$ indicate the observation of a number of previously unreported α emitters with energies reaching as high as 12 MeV. As discussed in the analysis and results section, α-particle energies above 11.5 MeV exhibited unrealistic derived implantation depths indicating that they corresponded to ternary fission events. In addition, the results presented in Fig. 8 suggest that isomeric states may account for most activities with energies greater than 10.6 MeV. Assuming this 10.6 MeV as a limit, comparing the energies and half-lives of these α emitters with known and predicted half-lives (Fig. 6) suggests that new activities with Z as high as 116 are being produced in these reactions. Any nonisomeric transitions with energies between 10.6 and 11.5 MeV would suggest even higher atomic numbers. First cross-section estimates imply that the cross sections are significantly higher than estimated by many models employing statistical decay calculations. This may reflect a confluence of several factors, i.e., shell effects leading to higher barriers and lower excitation energies of the relevant primary nuclei, the importance of microscopic fission dynamics, and β-decay feeding by neighboring nuclei. It is our hope that the present data provide an incentive and a basic road map for further work in this direction. This could include more narrowly focused experiments with such an active catcher array and/or with appropriately designed spectrometers [55,70]. We believe that a much improved active catcher array with higher granularity, better energy resolution, and linear energy response is realizable using single crystal diamond detectors and faster electronics. Such a detector would allow the establishment of parent-daughter relationships and searches for even smaller production rates.

ACKNOWLEDGMENTS

During the course of this research our colleague Z. Sosin died. He was a major contributor to the project and is greatly missed. We thank A. Staszczak, A. Afanasiev, V. Karpov. K. Zhao, S. Giuliani, and V. Zagrebaev (deceased), all of whom provided us with detailed tables of their theoretical results. We also would like to acknowledge very useful conversations and exchanges with S. Umar and H. Freiesleben. We thank the operations staff of the TAMU Cyclotron Institute for all of their efforts in support of this work. This work was supported by the United States Department of Energy under Grant No. DE-FG03- 93ER40773 and by The Robert A. Welch Foundation under Grant No. A0330 as well as by the National Science Center in Poland, Contract No. UMO-2012/04/A/ST2/00082.

[1] G. Hermann, Nature (London) **280**, 543 (1979).
[2] G. N. Flerov and G. M. Ter-Akopian, Rep. Prog. Phys. **46**, 817 (1983).
[3] P. Armbruster, Rep. Prog. Phys. **62**, 465 (1999).
[4] *Heavy Elements and Related New Phenomena*, edited by W. Greiner and R. K. Gupta (World Scientific, London, 1999).
[5] Y. T. Oganessian, V. K. Utyonkov, Y. V. Lobanov, F. S. Abdullin, A. N. Polyakov, R. N. Sagaidak, I. V. Shirokovsky, Y. S. Tsyganov, A. A. Voinov, G. G. Gulbekian, S. L. Bogomolov, B. N. Gikal, A. N. Mezentsev, S. Iliev, V. G. Subbotin, A. M. Sukhov, K. Subotic, V. I. Zagrebaev, G. K. Vostokin, M. G. Itkis, K. J. Moody, J. B. Patin, D. A. Shaughnessy, M. A. Stoyer, N. J. Stoyer, P. A. Wilk, J. M. Kenneally, J. H. Landrum, J. F. Wild, and R. W. Lougheed, Phys. Rev. C **74**, 044602 (2006).
[6] Yu Ts Oganessian and V. K. Utyonkov, Rep. Prog. Phys. **78**, 036301 (2015).
[7] J. Dechargé, J.-F. Berger, K. Dietrich, and M. S. Weiss, Phys. Lett. B **451**, 275 (1999).
[8] M. Bender, W. Nazarewicz, and P.-G. Reinhard, Phys. Lett. B **515**, 42 (2001).
[9] C. Y. Wong, Phys. Lett. B **41**, 451 (1972); Ann. Phys. (NY) **77**, 279 (1973).
[10] V. Pershina, T. Bastug, J. Anton, and B. Fricke, Nucl. Phys. A **787**, 381 (2007); Eur. Phys. J. D **45**, 87 (2007).
[11] Ch. E. Düllmann, W. Brüchle, R. Dressler, K. Eberhardt, B. Eichler, R. Eichler, H. Gäggeler, T. N. Ginter, F. Glaus, K. E. Gregorich, D. C. Hoffman, E. Jäger, D. T. Jost, U. W. Kirbach, D. M. Lee, H. Nitsche, J. B. Patin, V. Pershina, D. Piguet, Z. Qin, M. Schädel, B. Schausten, E. Schimpf, H.-J. Schött, S. Soverna, R. Sudowe, P. Thörle, S. N. Timokhin, N. Trautmann, A. Türler, A. Vahle, G. Wirth, A. B. Yakushev, and P. M. Zielinski, Nature (London) **418**, 859 (2002).
[12] M. Schädel, W. Brüchle, H. Gäggeler, J. V. Kratz, K. Summerer, and G. Wirth, G. Herrmann, R. Stakemann, G. Tittel, and N. Trautmann, J. M. Nitschke, E. K. Hulet, R. W. Lougheed, R. L. Hahn, and R. L. Ferguson, Phys. Rev. Lett. **48**, 852 (1982).
[13] P. Edwards, B. Krebs, P. Raithby, N. Long, A. Cheetham, and M. Schröder, Phil. Trans. R. Soc. A **373**, (2015).
[14] M. Bender, J. Phys.: Conf. Ser. **420**, 012002 (2013).
[15] O. V. Kiren, S. B. Gudennevar, and S. G. Bubbly, Rom. J. Phys. **57**, 1335 (2012).
[16] A. Staszczak, A. Baran, and W. Nazarewicz, Phys. Rev. C **87**, 024320 (2013).
[17] A. Q. Baran, M. Kowal, P.-G. Reinhard, L. M. Robledo, A. Staszczak, and M. Warda, Nucl. Phys. A **944**, 442 (2015).
[18] S. E. Agbemava, A. V. Afanasjev, T. Nakatsukasa, and P. Ring, Phys. Rev. C **92**, 054310 (2015).
[19] S. E. Agbemava, A. V. Afanasjev, D. Ray, and P. Ring, Phys. Rev. C **95**, 054324 (2017).
[20] C. I. Anghel and I. Silisteanu, Phys. Rev. C **95**, 034611 (2017).
[21] S. A. Giuliani, G. Martinez-Pinedo, and L. M. Robledo, Phys. Rev. C **97**, 034323 (2018).
[22] A. V. Karpov, V. I. Zagrebaev, Y. Martinez Palenzuela, and W. Greiner, Int. J. Mod. Phys. E **21**, 1250013 (2012).
[23] Y. Martinez-Palenzuela, L. Filipe Ruiz, A. Karpov, and W. Greiner, Bull. Russ. Acad. Sci. **76**, 1165 (2012).
[24] T. Marketin, L. Huther, and G. Martinez-Pinedo, Phys. Rev. C **93**, 025805 (2016).
[25] Y. T. Oganessian, V. K. Utyonkov, Y. V. Lobanov, F. S. Abdullin, A. N. Polyakov, I. V. Shirokovsky, Y. S. Tsyganov, G. G. Gulbekian, S. L. Bogomolov, B. N. Gikal, A. N. Mezentsev, S. Iliev, V. G. Subbotin, A. M. Sukhov, G. V. Buklanov, K. Subotic, M. G. Itkis, K. J. Moody, J. F. Wild, N. J. Stoyer, M. A. Stoyer, and R. W. Lougheed, Phys. Rev. Lett. **83**, 3154 (1999).
[26] Yu. Ts. Oganessian *et al.*, Sci. Am. **282**, 63 (2000).
[27] K. Morita, K. Morimoto, D. Kaji, H. Haba, K. Ozeki, Y. Kudou, T. Sumita, Y. Wakabayashi, A. Yoneda, K. Tanaka, S. Yamaki, R. Sakai, T. Akiyama, S.-I. Goto, H. Hasebe, M. Huang, T. Huang, E. Ideguchi, Y. Kasamatsu, K. Katori, Y. Kariya, H. Kikunaga, H. Koura, H. Kudo, A. Mashiko, K. Mayama, S.-I. Mitsuoka, T. Moriya, M. Murakami, H. Murayama, S. Namai, A. Ozawa, N. Sato, K. Sueki, M. Takeyama, F. Tokanai, T. Yamaguchi, and A. Yoshida, J. Phys. Soc. Jpn. **81**, 103201 (2012).
[28] J. H. Hamilton, S. Hofmann, and Y. T. Oganessian, J. Phys.: Conf. Ser. **580**, 012019 (2015).
[29] S. Hofmann, V. Ninov, F. P. Heßberger, P. Armbruster, H. Folger, G. Münzenberg, H. J. Schött, A. G. Popeko, A. V. Yeremin, S. Saro, R. Janik, and M. Leino, Z. für Physik A **354**, 229 (1996).
[30] V. Utyonkov, Y. Oganessian, S. Dmitriev, M. Itkis, K. Moody, M. Stoyer, D. Shaughnessy, J. Roberto, K. Rykaczewski, and J. Hamilton, EPJ Web Conf. **131**, 06003 (2016).
[31] Yu. Oganessian, J. Phys. Conf. Ser. **874**, 4848 (2017).
[32] V. I. Zagrebaev, A. Karpov, and W. Greiner, J. Phys.: Conf. Ser. **420**, 012001 (2013).
[33] V. I. Zagrebaev and W. Greiner, Phys. Rev. C **87**, 034608 (2013).
[34] J. Tian, X. Wu, K. Zhao, Y. Zhang, and Z. Li, Phys. Rev. C **77**, 064603 (2008).
[35] K. Zhao, Z. Li, Y. Zhang, N. Wang, Q. Li, C. Shen, Y. Wang, and X. Wu, Phys. Rev. C **94**, 024601 (2016)
[36] A. V. Karpov and V. V. Saiko, Phys. Rev. C **96**, 024618 (2017).
[37] C. Golabek, S. Heinz, W. Mittig, F. Rejmund, A. C. C. Villari, S. Bhattacharyva, D. Boilley, G. De France, A. Drouart, L. Gaudefroy, L. Giot, V. Maslov, M. Morjean, G. Mukherjee, Yu. Penionzkevich, P. Roussel-Chomaz, and C. Stodel, Eur. Phys. J. A **43**, 251 (2010).
[38] T. Welsh, W. Loveland, R. Yanez, J. S. Barrett, E. A. McCutchan, A. A. Sonzogni, T. Johnson, S. Zhu, J. P. Greene, A. D. Ayangeakaa, M. P. Carpenter, T. Lauritsen, J. L. Harker, W. B. Walters, B. M. S. Amro, and P. Copp, Phys. Lett. B **771**, 119 (2017).
[39] C. Golabek and C. Simenel, Phys. Rev. Lett. **103**, 042701 (2009).
[40] D. J. Kedziora and C. Simenel, Phys. Rev. C **81**, 044613 (2010).
[41] J. V. Kratz, W. Loveland, and K. J. Moody, Nucl. Phys. A **944**, 117 (2015).
[42] M. Schädel, EPJ Web Conf. **131**, 04001 (2016).
[43] K. D. Hildenbrand, H. Freiesleben, F. Pühlhofer, W. F. W. Schneider, R. Bock, D. V. Harrach, and H. J. Specht, Phys. Rev. Lett. **39**, 1065 (1977).
[44] H. Gäggeler, N. Trautmann, W. Brüchle, G. Herrmann, J. V. Kratz, P. Peuser, M. Schädel, G. Tittel, G. Wirth, H. Ahrens, H. Folger, G. Franz, K. Summerer, and M. Zendel, Phys. Rev. Lett. **45**, 1824 (1980).
[45] H. Jungclas, D. Hirdes, R. Brandt, P. Lemmertz, E. Georg, and H. Wollnik, Phys. Lett. B **79**, 58 (1978).
[46] H. Freiesleben, K. D. Hildenbrand, F. Pühlhofer, W. F. W. Schneider, and R. Bock, Z. Physik A **292**, 171 (1979).
[47] C. Reidel and W. Norenberg, Z. Physik A **290**, 385 (1979).
[48] J. V. Kratz, W. Brüchle, H. Folger, H. Gäggeler, M. Schädel, K. Sümmerer, G. Wirth, N. Greulich, G. Herrmann, U. Hickmann, P. Peuser, N. Trautmann, E. K. Hulet, R. W. Lougheed, J. M.

Nitschke, R. L. Ferguson, and R. L. Hahn, Phys. Rev. C **33**, 504 (1986).
[49] H. Gäggeler, W. Brüchle, J. V. Kratz, M. Schädel, K. Summerer, H. Wewber, G. Wirth, and G. Herrmann, Nucl. Inst. & Meth. A **188**, 367 (1981).
[50] N. Trautmann and M. Weiss, Phys. Rev. Lett. **41**, 469 (1978).
[51] J. V. Kratz, M. Schädel, and H. W. Gäggeler, Phys. Rev. C **88**, 054615 (2013).
[52] Yi Zhu and J. C. Pei, Phys. Scr. **92**, 114001 (2017).
[53] C-J. Xia, B.-Xi Sun, E.-G. Zhao, and S.-G. Zhou, Sci. China - Phys. Mech. Astron. **54**, 109 (2011).
[54] T. W. O'Donnell, F. D. Becchetti, J. Brown, J. W. Jänecke, M. Y. Lee, R. S. Raymond, D. A. Roberts, R. S. Tickle, H. C. Griffin, and R. M. Ronningen, Nucl. Instr. Meth. A **422**, 513 (1999); T. W. O'Donnell, Ph.D thesis, University of Michigan, 2000.
[55] M. Barbui, Ph.D. thesis, University of Padova, 2006.
[56] M. Barbui, D. Fabris, M. Lunardon, S. Moretto, G. Nebbia, S. Pesente, G. Viesti, M. Cinausero, G. Prete, V. Rizzi, K. Hagel, S. Kowalski, J. B. Natowitz, L. Qin, R. Wada, and Z. Chen, Nucl. Inst. And Meth. B **268**, 20 (2010).
[57] Z. Majka, M. Barbui, F. Becchetti, G. Chubaryan, M. Cinausero, D. Fabris, G. Giuliani, H. Griffin, K. Hagel, J. Kallunkathariyil, E.-J. Kim, S. Kowalski, P. Lasko, M. Lunardon, T. Materna, S. Moretto, R. Murthy, J. Natowitz, G. Nebbia, T. O'Donnel, S. Pesente, R. Płaneta, G. Prete, L. Quin, V. Rizzi, P. Sahu, K. Schmidt, G. Souliotis, Z. Sosin, G. Viesti, R. Wada, J. Wang, A. Wieloch, S. Wuenschel, and H. Zhen, Acta Physica Polonica **45**, 279 (2014).
[58] A. Wieloch, M. Adamczy, M. Barbui, N. Blando, G. Giuliani, K. Hagel, E. J. Kim, S. Kowalski, Z. Majka, J. Natowitz, K. Pelczar, R. Płaneta, K. Schmidt, Z. Sosin, S. Wuenschel, K. Zelga, and H. Zheng, EPJ Web Conf. **117**, 01003 (2016).
[59] P. Ren, W. Lin, R. Wada, X. Liu, M. Huang, G. Tian, F. Luo, Q. Sun, Z. Chen, G. Xiao, R. Han, F. Shi, and B. Gou, Nucl. Sci. Tech. (Shanghai) **28**, 145 (2017).
[60] J. F. Zeigler, M. D. Zeigler, and J. P. Biersack, Nucl. Inst. & Meth. B **268**, 1818 (2010).
[61] J. Allison *et al.*, Nucl. Inst. and Meth. A **835**, 186 (2016).
[62] M. Mutterer, Yu. N. Kopatch, S. R. Yamaledtinov, V. G. Lyapin, J. von Kalben, S. V. Khlebnikov, M. Sillanpää, G. P. Tyurin, and W. H. Trzaska, Phys. Rev. C **78**, 064616 (2008).
[63] K.-H. Schmidt, C.-C. Sahm, K. Pielenz, and H.-G. Clerc, Z. Physik A **316**, 19 (1984).
[64] https://www.bnl.gov/NST/NNDC.php.
[65] http://www.nrv.jinr.ru/.
[66] V. E. Viola, Jr. and G. T. Seaborg, J. Inorg. Nucl. Chem. **28**, 741 (1966).
[67] I.-Y. Lee, Nucl. Phys. A **520**, c641 (1990).
[68] R. Brun and F. Rademakers, Nucl. Inst. & Meth. Phys. Res. A **389**, 81 (1997), See also http://root.cern.ch/.
[69] https://wwww.r-project.org/.
[70] M. Schädel, Eur. Phys. J. D **45**, 67 (2007).